RC Frame Analysis with a New Damage-following Model

J.P. Almeida
EUCENTRE – European Centre for Training and Research in Earthquake Engineering, Pavia, Italy

S. Das
Indian Institute of Technology Guwahati, India

R. Pinho
University of Pavia, Italy

SUMMARY:
Experimentally tested RC columns demonstrate that, for large inelastic demands under cyclic loading, damage concentrates within a finite member length around the section of maximum moment. This region length is shown to increase significantly with compressive axial load. The present work addresses the need to incorporate such finding in inelastic analyses of frame buildings and bridges, in order to reconcile the simulation of local (moment-curvature) and global (drift-lateral load) responses. The proposed model combines: (i) a recently developed adaptive force-based beam element, which ensures simultaneously a high degree of accuracy for hardening behaviour and an objective response during the post-peak phase(s); (ii) a new method to estimate the damaged region length, based on the distribution of the steel strains along the compressed longitudinal reinforcement. Numerical tests and comparison with experimental results under distinct values of axial load ratio show an overall satisfactory performance of the model.

Keywords: Damage, Regularization, Force-based, Axial Load, Column.

1. INTRODUCTION

The dynamic analysis of reinforced concrete (RC) buildings or bridges under earthquake loading is generally carried out with beam-column elements, which should thus be able to duly take into account the inelastic behaviour of the actual member.

The evolution of inelasticity can be tackled in two ways: by assuming that it concentrates within a chosen length in a pre-defined location of the member, or alternatively by allowing it to spread throughout the element. In the former case – lumped plasticity models, a value for the plastic hinge length is directly or indirectly assumed. In the latter category – distributed plasticity models, the inelasticity can spread throughout the member and therefore *a priori* estimations of the plastic hinge length are not required. That only holds true before the occurrence of softening sectional response, or if such branch does not take place at all; during post-peak phases of behaviour, a damaged region length should be defined in order to obtain regularized responses, as discussed below.

The present proposal advances the current knowledge by associating a recent adaptive force-based beam element, used to obtain regularized softening responses, with a new method to predict the damaged region length of RC members. The latter is not based on traditional closed-form expressions, but rather on the evaluation of the steel strain distribution along the compressed longitudinal reinforcement. Finally, the previous approach is tested and compared with experimental results.

2. AXIAL LOAD AND DAMAGED REGIONS IN RC MEMBERS

2.1. Plastic Hinge Length vs. Damaged Region Length

The term 'plastic hinge length' is still widely used to interchangeably describe two distinct quantities: (i) a conventional and fictitious parameter that accounts indirectly for the effects of shear, bond-slip, etc, and from which the inelastic member displacement can be computed based on an assumed curvature distribution; (ii) an actual physical 'damaged region length', wherein major member damage concentrates, such as: cover spalling, yielding of longitudinal steel, crushing of concrete core, buckling of rebars, yielding of transversal reinforcement. The latter is also sometimes called 'critical region length' or ''ductile detailing length' [Pam and Ho, 2009], since it indicates the member region that should be effectively confined by transverse reinforcement in order to achieve a desired performance level. A distinction between 'length of plastification' and 'plastic hinge length' is also explicitly addressed by Fardis [2009].

Besides being conceptually different, in general the two definitions above do not correspond to the same quantitative value: even subtle differences can have a significantly impact on the accuracy of the analyses. The misuse of terminology, which often occurs within the technical community itself, holds back the development of a more insightful understanding of RC frame modelling. The authors themselves often capitulate to the usage of 'plastic hinge length' as an 'umbrella definition', established in the early days of Earthquake Engineering; however, in the present work the aforementioned separation is respected.

2.2. The Influence of Axial Load

A number of factors affect the damaged region length: axial load ratio, moment gradient, mechanical properties of longitudinal and transversal steel, concrete strength, level of shear stress, level of confinement, etc. In particular, and up until recently, the influence of the axial load was not clearly understood, probably due to the fact that it is not so apparent in low axial load ranges. That was reflected in an overwhelming neglect of the axial load in the majority of available formulas for plastic hinge length.

For instance, Park *et al.* [1982] suggested the use of $0.4h$, where h is the overall depth of a column. Another widely used expression is the formula by Paulay and Priestley [1992], $0.08L + 0.022d_b f_y$ (yield strength f_y in MPa), where L is the height of a cantilever column and d_b is the diameter of the longitudinal rebar.

Nevertheless, recent research showed that the damaged region length increases with compressive axial load, and that such increase can be quite meaningful for moderate to high axial load ratios [Bae and Bayrak, 2008; Pam and Ho, 2009]. Hence, more recent formulas for the plastic hinge length (and for the damaged region length) incorporate such finding, which is also considered in the present work.

As an alternative to the typical closed-form expressions used to compute the plastic hinge length, Bae and Bayrak [2008] proposed a method, called 'Concrete Compression Strain Method', which also accounts for the effect of the axial load. It is based on experimental observations showing that the damaged region starts to form after the maximum moment capacity is reached, concentrating within a finite member length around it. The crucial step in the method involves plotting the most compressed longitudinal bar strain profile along the column length (when the maximum moment occurs, as stated before), and subsequently identifying the length of the region in which such bar is yielding; such rebar yielding length is denoted as L_y.

A similar rationale is used for the procedure developed herein, which the following section addresses in detail.

3. NEW DAMAGE-FOLLOWING MODEL

3.1. Proposed Method for Computation of Damaged Region Length

Bae and Bayrak [2008] implemented their plastic hinge model in a computer program for the analysis of individual cantilevers. Distinctly, a new procedure is proposed for incorporation into a finite element computer code previously developed by the authors. It analyses frame structures under static or cyclic loading, making use of distributed plasticity elements.

As discussed in section 2.1., the plastic hinge length and the damaged region length are distinct concepts. The latter should be used to regularize the response in the context of distributed plasticity elements – in particular when force-based elements, which strictly satisfy equilibrium, are employed. Consequently, the procedure by Bae and Bayrak [2008], which directs to plastic hinge analysis, requires adjustment.

The criterion proposed herein is simply to add the rebar yielding length L_y to a value of $0.4h$. The latter term thus stands as a 'minimum' value of the damaged region length, while L_y reflects the influence of a number of factors such as the axial load, the moment gradient, or the mechanical properties of the longitudinal reinforcement.

The fact that the damaged region length can be estimated (at least approximately) when the maximum moment capacity is attained, aligns very conveniently with the need to regularize the post-peak softening response from that point on and to keep the physical meaningfulness of the results. The advantage of the current method is that it is not based on the use of a closed-form expression, but rather on the direct and continuous monitoring of a parameter that varies during the response and thus provides updated information on the condition of the member.

3.2. Adaptive Force-based Element for Regularized Response

The versatile 'adaptive force-based formulation' developed by Almeida *et al.* [2012], which is based on an automatic and computationally efficient commutation between integrations schemes, is used for the implementation of the current method. It ensures a high degree of accuracy for hardening behavior and, simultaneously, an objective regularized response during the post-peak phase(s).

Additionally, it frees the analyst from the difficult task of deciding, *a priori*, whether to use a standard or a regularized integration approach: the element employs the standard Gauss-Lobatto integration scheme during the hardening phase and continuously checks for the occurrence of softening at the extreme integration points (IPs). In the latter case, i.e., when the maximum moment capacity is overcome, the integration weights commute to those provided by an interpolatory quadrature rule using an appropriate value of the damaged region length.

The length of the region where the compressive longitudinal bars are yielding, L_y, is computed automatically from a piecewise cubic interpolation between the vector assembling the controlling rebar compression strains at every IP along the element, and the vector assembling the bending moments at every IP. Therefore, the accuracy of the above interpolation increases when the number of IPs per element also increases.

4. APPLICATIONS

4.1. Specimen Details and Modelling Approach

In order to illustrate the aforementioned method, the experimental tests of two full-scale columns by Bae [2005] are modelled. The specimens – identified by the acronyms S24-2UT and S24-5UT – were tested under moderate and high axial load levels, and reversed lateral cyclic displacements.

Table 4.1. Details of test specimens

Specimen	Concrete	Longitudinal steel				Transversal steel			
	f_c' [MPa]	Diameter [mm]	Number	ρ_{yl} [%]	f_{yl} [MPa]	Diameter [mm]	spacing s_h [mm]	ρ_s [%]	f_{yh} [MPa]
S24-2UT	43.4	22.2	12	1.25	503	12.7	95	2.03	427
S24-5UT	41.4	22.2	12	1.25	400	12.7	152	1.27	434

The columns' height is 3.048 m and their square cross-sectional dimensions are 609.6 × 609.6 mm. The specimens were axially loaded with $P = 0.5P_0$ and $P = 0.2P_0$, respectively. P_0 stands for the nominal axial load capacity as per ACI 318-05 [2005] and is given by $P_0 = 0.85f_c'(A_g - A_s) + f_{yl} A_s$, where: f_c' is the compressive strength of concrete, A_g is the gross area of concrete section, A_s is the area of tension reinforcement, and f_{yl} is the yield stress of longitudinal reinforcement. Further details on the test specimens can be found in Table 4.1, as well as in Bae [2005].

Shear deformation is not expected to play a relevant role since the shear span-to-depth ratio is relatively large (=5). On the other hand, the latter value – in association with the large axial load ratio, may indicate the importance of geometrical nonlinear effects. These were accounted for through a corotational formulation.

One force-based element is used to model each specimen [Calabrese *et al.*, 2010]. The element integration assembles the response of the member from several controlling sections and is performed with a Gauss-Lobatto scheme with five or seven IPs, or an adaptive scheme with 7 IPs [Almeida *et al.*, 2012], see discussion below. At the IP level, the corresponding sectional response is evaluated through a refined layer approach, wherein different uniaxial constitutive laws are assigned to each material.

In general, concrete tested in large members depict a lower apparent unconfined compression strength f_{co}' than the control-cylinder strength f_c' (see Table 4.1). Consequently, an assumed $f_{co}' = 0.9f_c'$ is assigned to the concrete cover layers. The unconfined concrete strain ε_{co} is considered to be 0.002, as usual, and the concrete Young's modulus is estimated as $E_c = 5000\times(f_{co}')^{1/2}$. The tensile strength is computed with the expression $f_t' = 0.34\times(f_{co}')^{1/2}$.

The compressive concrete stress is given by the equation suggested by Popovics [1973], while a linear response is assumed for tensile behaviour up to tension resistance, followed by an exponential decay.

Confinement effects on the concrete core due to the transverse reinforcement can be simulated by a confinement factor k_c. Herein, the confined compression strength and corresponding strain are obtained through $f_{cc}' = k_c f_{co}'$ and $\varepsilon_{cc} = \varepsilon_{co}\,[1 + 5\times(k_c - 1)]$, respectively. The confinement factor k_c is evaluated with the well-known model of Mander *et al.* [1988], resulting in $k_c = 1.479$ for specimen S24-2UT and $k_c = 1.301$ for specimen S24-5UT. The previous parameters define the model assigned to the concrete core layers.

Finally, the longitudinal reinforcing steel is modelled with a bilinear stress–strain relationship with elastic modulus $E_s = 200$ GPa, 1% strain-hardening ratio, and yield stress as depicted in Table 4.1.

4.2. Simulation with Fibre Frame Models

Figures 1 and 2 show the experimental and numerical moment-curvature curves, where the latter are obtained with the model described in the previous section. It should be noted that the experimental curvatures were calculated from the displacement readings measured by the upper and lower linear potentiometers located at the most damaged region [Bae, 2005]. This last author indicates that the procedure used to compute the backbones curves was adopted from FEMA 356 [2000].

The comparison indicates a satisfactory simulation. Furthermore, the effect of the axial load in increasing the flexural capacity and reducing the available sectional curvature ductility is apparent.

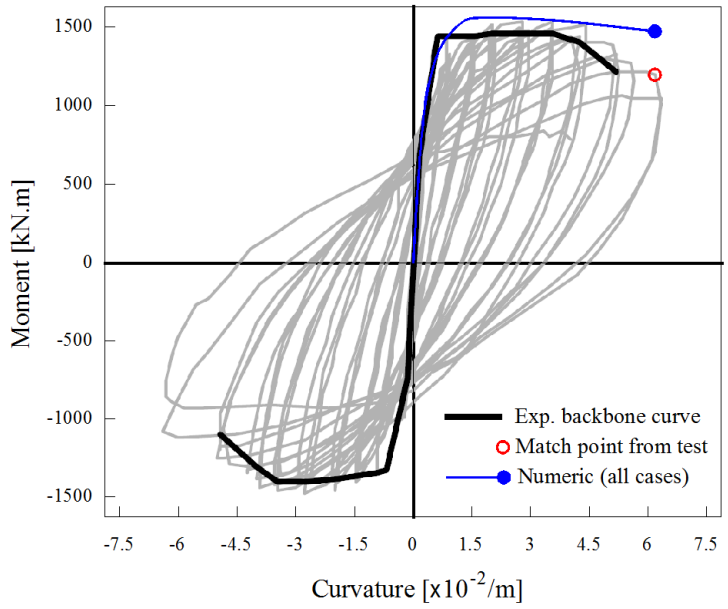

Figure 1. Moment – Curvature response at most damaged region, at the base of specimen S24-2UT ($P = 0.5P_0$).

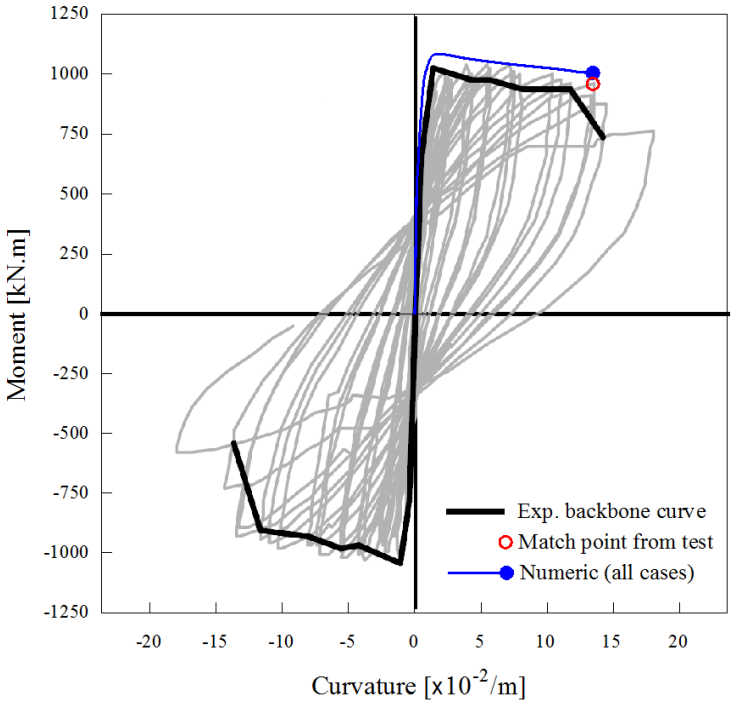

Figure 2. Moment – Curvature response at most damaged region, at the base of specimen S24-5UT ($P = 0.2P_0$).

At the member level, Figures 3 and 4 display the response of a force-based element with a Gauss-Lobatto integration scheme. Such option represents the most commonly used approach for the simulation of inelastic behaviour with distributed plasticity models. The cases of five and seven IPs (controlling sections) are studied, which corresponds approximately to lower and upper bounds employed in practical structural analysis.

It can be seen that the imposed maximum top lateral displacement depends on the specimen (S24-2UT or S24-5UT) and number of IPs (five or seven). There is also a circle identifying experimental drift-load points, denoted as ‘Match point from test’.

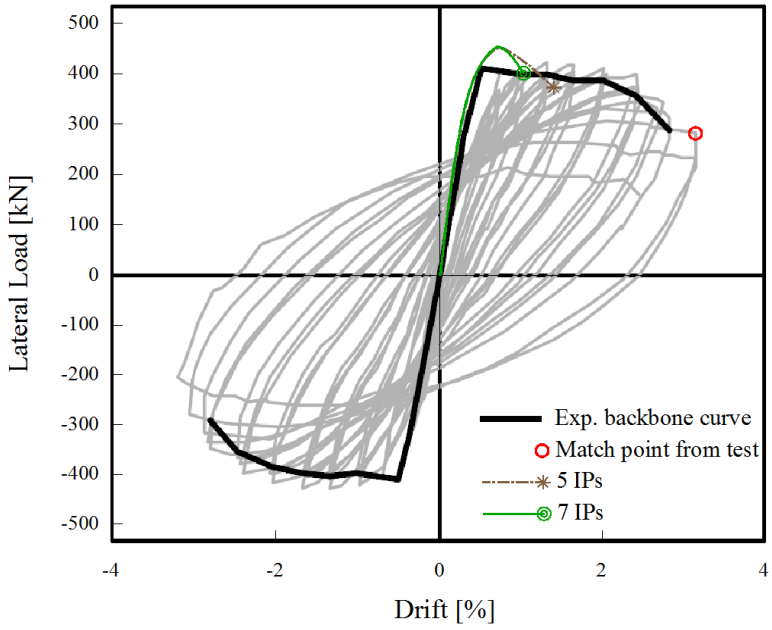

Figure 3. Drift - Load response of specimen S24-2UT ($P = 0.5P_0$) using typical Gauss-Lobatto integration.

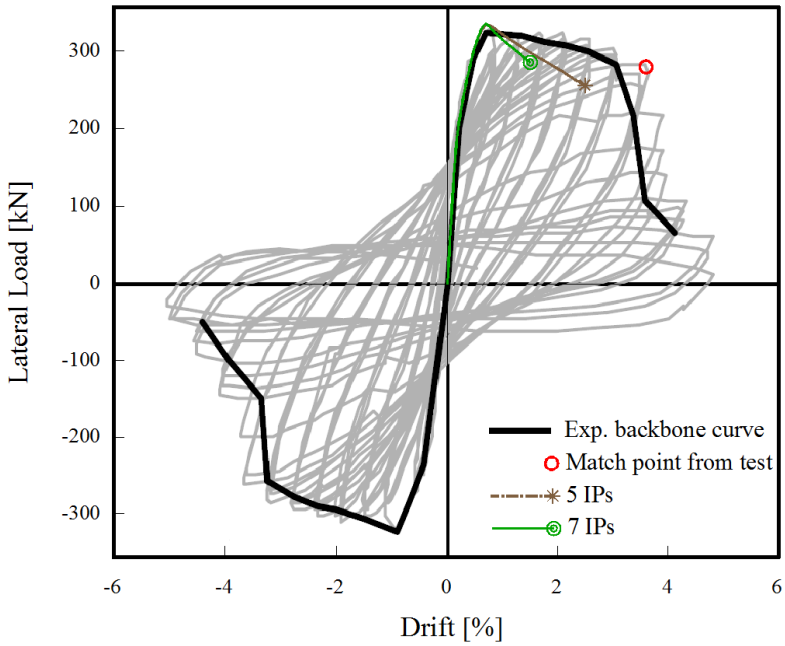

Figure 4. Drift - Load response of specimen S24-5UT ($P = 0.2P_0$) using typical Gauss-Lobatto integration.

All the above-mentioned drift levels correspond to attaining the same base sectional curvature indicated in Figures 1 and 2. The fundamentally distinct values of the maximum top displacements with five and seven IPs, as well as the displacements corresponding to the 'Match point from test', are worrying. They serve as a clear evidence of the difficulty in establishing a connection between the simulated local and global levels of behaviour.

The previous poor performances are due to localized responses along the post-peak branches, wherein the finite element problem becomes ill-posed, and indirectly defines a region wherein inelasticity concentrates. The length of that region is defined by the integration weight of the Gauss-Lobatto IP where the maximum moment capacity is surpassed; hence, it is an artificial and unintended

consequence of the numerical integration scheme adopted, and does not necessarily reflect the damaged region length observed in actual tested specimens. In order to establish such link, an appropriately computed damaged region length must be imposed, as investigated in the next section.

4.3. Response with Damage-following Model

The adaptive force-based element developed by Almeida *et al.* [2012] is now employed, in association with distinct expressions for the damaged region length: (i) the expression by Park *et al.* [1982], indicated in section 2.2.; (ii) the expression by Paulay and Priestley [1992], also recalled in section 2.2.; (iii) the suggested method to compute the damaged region length, proposed in section 3.1.

Seven IPs are defined for the element integration, which represents a sufficiently large number for accurate interpolation of the longitudinal rebar compressive strain, as discussed in section 3.2.

The values of the damaged region lengths obtained with the three alternative approaches are summarised in Table 4.2. It also includes, for comparative purposes, the equivalent regularization lengths implicitly assumed when five or seven Gauss-Lobatto IPs are used.

Table 4.2. Damaged region lengths as predicted by different models, and implicit in Gauss-Lobatto quadrature

Specimen	Paulay & Priestley	Park *et al.*	Proposed Model	5 Gauss-Lobatto IPs	7 Gauss-Lobatto IPs
S24-2UT	0.804 *h*	0.4 *h*	0.978 *h*	0.25 *h*	0.119 *h*
S24-5UT	0.721 *h*	0.4 *h*	0.442 *h*	0.25 *h*	0.119 *h*

The drift-lateral load response curves are shown in Figures 5 and 6. Once again, the same principle was employed to define the distinct values of the final imposed drifts: they all correspond to attaining the same values of the curvatures at the base section, depicted in Figures 1 and 2.

The main conclusions that can be drawn from Figures 5 and 6 are: (i) for specimen S24-2UT, tested under high axial load ratio, the use of the expression by Park *et al.* [1982] results in a very significant underestimation of the drift capacity. On the other hand, regularizing the response with the equation by Paulay and Priestley [1992] yields a more acceptable prediction; (ii) for specimen S24-5UT, tested under moderate axial load ratios, the expression by Park *et al.* [1982] yields a good agreement, whilst the proposal by Paulay and Priestley [1992] produces an unsafe overestimation of the drift capacity; (iii) the proposed model simulates very efficiently the drift capacity of both tested specimens.

Furthermore, it is noted that the response is exactly identical up to the peak. In other words, the distinct concentrations of curvatures for the different cases take place exclusively along the softening branch. For damaged region lengths smaller than the length where damage actually concentrates (see Table 4.2), the localization is more intense and the drift capacity is underestimated. Similarly, an overestimation of the drift capacity can also occur when the actual damaged region length is overvalued.

Although the results obtained with the proposed model are satisfactory, a more thorough validation should be carried out by comparison with other experimental tests. The ultimate goal should always be the development of more reliable methods to compute the damaged region lengths.

Finally, it should be acknowledged that the drift-lateral load simulation is not overly satisfactory (in terms of prediction of the resisting force or the post-peak branch of the response). Using a totally different modelling approach (lumped plasticity), Bae and Bayrak [2008] obtained similar results, which proves that the discrepancy is not due to (or specific to) fibre modelling approaches. The causes of such partial mismatch should be further and deeply investigated, but they stand out as a warning to the existing numerical difficulties in accurately reproducing a simple monotonic inelastic member response.

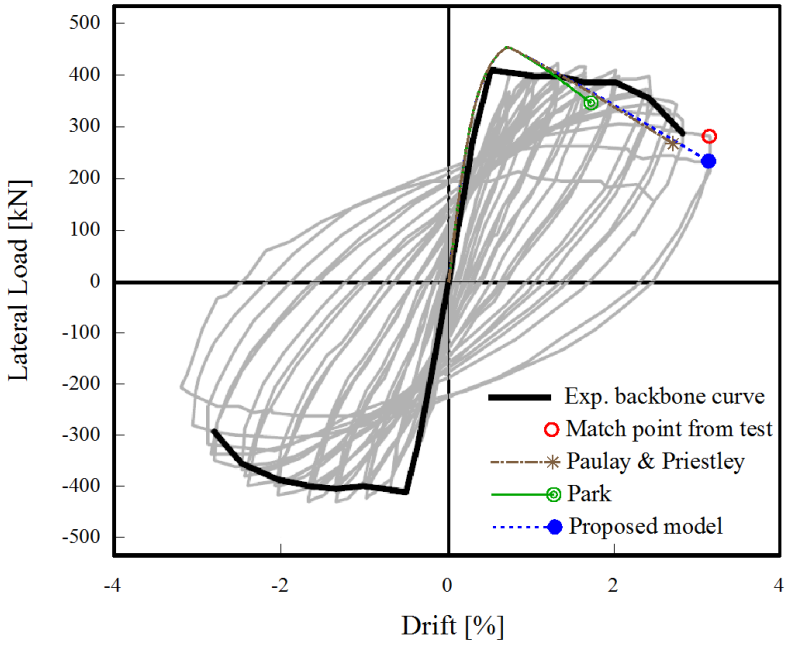

Figure 5. Drift - Load response of specimen S24-2UT ($P = 0.5P_0$) with regularized schemes.

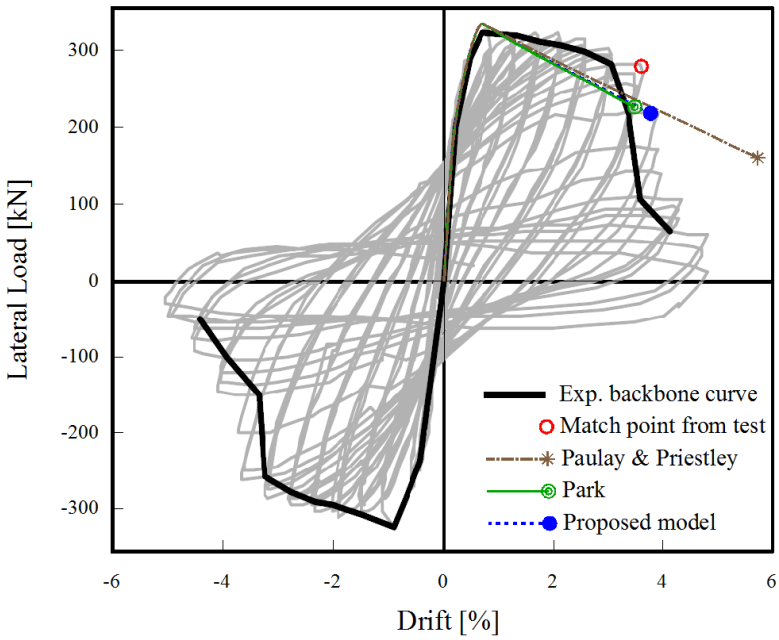

Figure 6. Drift - Load response of specimen S24-5UT ($P = 0.2P_0$) with regularized schemes.

5. CONCLUSIONS

The simulation of highly axially loaded RC members can pose complicated challenges to the engineer. On the one hand, recent research has shown that the region where damage concentrates can increase considerably under large axial load ratios. However, the majority of existing expressions for predicting the damaged region length (which are often, and incorrectly, interchangeably used with expressions for the plastic hinge length), do not yet acceptably model this feature. On the other hand, high axial loads tend to induce a softening type of response, giving rise to non-objective concentration of curvatures in the most strained sections.

The regularization of the previous behavior is herein achieved through the use of a recently developed adaptive force-based beam element that always ensures an objective response, as well as an optimization of the corresponding order of accuracy. Further, it is associated herein with a new method to estimate the damaged region length, based on the distribution of the steel strains along the compressed longitudinal reinforcement. The latter evolve during the inelastic response, and should thus prove more versatile than fixed closed-form expressions to represent it.

Numerical simulations and comparison with experimental results of specimens tested under distinct values of axial load ratios show an overall satisfactory performance of the model.

ACKNOWLEDGEMENTS

The authors would like to acknowledge the support provided by the European Commission through the financing of the FP7 research programmes SHARE and SYNER-G, under the framework of which this work has been partially funded.

REFERENCES

ACI Committee 318 (2005). Building Code Requirements for Structural Concrete (ACI 318-05) and Commentary (318R-05), American Concrete Institute, Farmington Hills, MI, US.

Almeida, J.P., Das, S. and Pinho, R. (2012). Adaptive force-based frame element for regularized softening response. *Computers and Structures* (in press)

Bae, S. (2005). Seismic Performance of Full-scale reinforced concrete columns. *PhD Thesis*. University of Texas at Austin.

Bae, S. and Bayrak, O. (2008). Plastic hinge length of reinforced concrete columns. *ACI Structural Journal* **105:3**,290-300.

Calabrese, A., Almeida, J.P. and Pinho, R. (2010). Numerical issues in distributed inelasticity modeling of RC frame elements for seismic analysis. *Journal of Earthquake Engineering* **14(S1)**,38-68.

Fardis, M.N. (2009). Seismic Design, Assessment and Retrofitting of Concrete Buildings, Springer.

Federal Emergency Management Agency (2000). Prestandard and Commentary for the Seismic Rehabilitation of Buildings, FEMA 356, Washington, DC, US.

Mander, J.B., Priestley, M.J.N. and Park, R. (1988). Theoretical stress-strain model for confined concrete. *Journal of Structural Engineering* **114:8**,1804-1826.

Pam, H.J. and Ho, J.C.M. (2009). Length of critical region for confinement steel in limited ductility high-strength reinforced concrete columns. *Engineering Structures* **31:12**,2896-2908.

Park, R., Priestley, M.J.N. and Gill, W.D. (1982). Ductility of square-confined concrete columns. *Journal of Structural Division ASCE* **108:4**,929-950.

Paulay, T., and Priestley, M.J.N. (1992). Seismic Design of Reinforced Concrete and Masonry Buildings, John Wiley and Sons, New York, US.

Popovics, S. (1973). A numerical approach to the complete stress-strain curves for concrete. *Cement and Concrete Research* **3:5**,583-599.